J Physiol (2003), **553.1**, *pp.* 49–63

DOI: 10.1113/jphysiol.2003.047746
www.jphysiol.org

Journal of Physiology

Preservation of motor neuron Ca^{2+} channel sensitivity to insulin-like growth factor-1 in brain motor cortex from senescent rat

Hongqu Shan*, María Laura Messi*, Zhenlin Zheng*, Zhong-Min Wang* and Osvaldo Delbono*†‡

**Department of Physiology and Pharmacology, †Department of Internal Medicine, Gerontology and ‡Neuroscience Program, Wake Forest University School of Medicine, Winston-Salem, North Carolina 27157, USA*

Despite the multiple effects on mammals during development, the effectiveness of the insulin-like growth factor-1 (IGF-1) to sustain cell function and structure in the brain of senescent mammals is almost completely unknown. To address this issue, we investigated whether the effects of IGF-1 on specific targets are preserved at later stages of life. Voltage-gated Ca^{2+} channels (VGCC) are well-characterized targets of IGF-1. VGCC regulate membrane excitability and gene transcription along with other functions that have been found to be impaired in the brain of senescent rodents. As the voluntary control of movement has been reported to be altered in the elderly, we investigated the expression, function and responsiveness of high (HVA)- and low-voltage-activated (LVA) Ca^{2+} channels to IGF-1, using the whole-cell configuration of the patch-clamp and RT-PCR in the specific region of the rat motor cortex that controls hindlimb muscle movement. We detected the expression of α_{1A}, α_{1B} and α_{1E} genes encoding the HVA Ca^{2+} channels P/Q, N and R, respectively, but not α_{1C}, α_{1D}, α_{1S} encoding the L-type Ca^{2+} channel in this region of the brain cortex. IGF-1 enhanced Ca^{2+} channel currents through P/Q- and N-type channels but not significantly through the R-type or LVA channels. IGF-1 enhanced the amplitude but did not modify the voltage dependence of Ca^{2+} channel currents in young (2- to 4-week-old), young adult (7-month-old) and senescent (28- to 29-month-old) rats. These results support the concept that despite the reported decrease in circulating (liver) and local (central nervous system) production of IGF-1 with ageing, key neuronal targets such as the VGCC remain responsive to the growth factor throughout life.

(Received 20 May 2003; accepted after revision 1 September 2003; first published online 5 September 2003)
Corresponding author O. Delbono: Department of Physiology and Pharmacology, Wake Forest University School of Medicine, Medical Center Boulevard, Winston-Salem, NC 27157, USA. Email: odelbono@wfubmc.edu

The insulin-like growth factor-1 (IGF-1) and its receptor IGF-1R are expressed in the central nervous system (Marks *et al.* 1991; Bondy *et al.* 1992) and play a central role in dendritic growth (Niblock *et al.* 2000), myelination (Florini *et al.* 1996; Ye *et al.* 2002), neuronal survival (Chrysis *et al.* 2001; Niikura *et al.* 2001) and adult stem-cell differentiation (Brooker *et al.* 2000), among other functions. Systemic IGF-1 exerts an effect on the brain as demonstrated by its ability to cross the blood–brain barrier and induce neurogenesis in adult rats (Aberg *et al.* 2000). The age-related decrease in pulsatile secretion of growth hormone in humans (Ho *et al.* 1987) and rodents (Sonntag *et al.* 1980) is paralleled by decreased levels of IGF-1 in blood (Ho *et al.* 1987). This may result in impairments of the IGF-1-dependent effects described above on the central nervous system at later stages of life. The requirement for a prolonged administration of growth hormone (GH) to ameliorate the age-related decline in cognitive function in rats (Sonntag *et al.* 2000) suggests that alterations in the GH–IGF1–IGF1R axis occur in mammalian ageing brain. Despite the multiple effects of IGF-1 during development, its role and effectiveness to sustain function in the ageing brain from senescent mammals is almost completely unknown. To address this issue, it is relevant to determine whether effects of IGF-1 on specific targets are preserved at later stages of life.

Voltage-gated Ca^{2+} channels (VGCC) are well-characterized targets of IGF-1. VGCC regulate membrane excitability and gene transcription among other functions (Berridge *et al.* 2000). In the present study, we investigated the ability of IGF-1 to modulate VGCC expressed in pyramidal neurons of the layer V of the brain motor cortex involved in the control of hindlimb movement in young (2- to 4-week-old), adult (7-month-old) and senescent (28- to 29-month-old) rats. These neurons encode functional muscle synergies in primates (Holdefer & Miller, 2002) with obvious effects on voluntary control of movement and posture by their influence on spinal cord motor neurons located in the lateral part of the lamina IX or interneurons that project to them. Whether motor cortex controls either high level features of limb movement (Georgopoulos *et al.* 1982) or muscle activation directly in voluntary movement (Todorov, 2000)

is debatable at the present time (Scott, 2000). However, the influence of neocortex neurons on various targets depends on the firing behaviour of pyramidal neurons (Chagnac-Amitai *et al.* 1990; Connors & Gutnick, 1990) that depends in turn on the ionic currents that shape action potentials (Stewart & Foehring, 2001). As there is specificity in the interaction of VGCC with Ca^{2+} firing behaviour in neocortical pyramidal neurons (Pineda *et al.* 1998), it is obvious that changes in the population of VGCC or their sensitivity to IGF-1 can account for alterations in limb movement or directly on muscle activation in voluntary movement. Functional and structural decline in the neuromuscular system with ageing have been recognized as causes of impairment in physical performance and loss of independence in the elderly (Delbono, 2003). As the voluntary control of movement and posture have been reported to be altered in the elderly (Leonard *et al.* 1997; Krampe, 2002), we investigated the expression, function and responsiveness of high- and low-threshold VGCC to IGF-1. For this, we used the whole-cell configuration of the patch-clamp and molecular techniques in the specific region of the rat motor cortex that controls hindlimb muscle movement.

METHODS

Localization of hindlimb cortex area of the brain by electrical stimulation mapping

Fisher344XBN rats (2–3 months old, $n = 5$) were anaesthetized using a combination of ketamine (100 mg ml^{-1}) and xylazine (20 mg ml^{-1}). A volume of 0.1–0.15 ml of the mixture per 100 g rat was injected I.P. with supplemental doses of one-quarter of the initial dose as needed. No assisted respiration was needed during the procedure. Animals did not exhibit spontaneous movements or evidence of pain. Animal handling and procedures followed an approved protocol by the Animal Care and Use Committee of Wake Forest University School of Medicine. At the end of the experiments, rats were killed by an overdose of the anaesthetics. Procedures to determine the brain cortex region involved in the control of hindlimb movement followed published methods (Neafsey *et al.* 1986).

Identification of pyramidal neurons from layer V of the rat brain motor cortex

The identification of pyramidal neurons from layer V of the brain motor cortex was performed in whole-cell voltage-clamp configuration by delivering Lucifer yellow via the patch-clamp glass pipette. We stained 15, 10 and 12 cells from 2- to 4-week-old, 7- and 28- to 29-month-old rats, respectively. Fluorescent images were digitized using a CCD camera EEV37 (Photometrix, Tucson, AZ, USA) controlled by Isee software (Inovision, Durham, NC, USA). This procedure was applied to a limited number of cells. The remaining cortical motor neurons were identified by their typical location in motor cortex, pyramidal shape and large size visualized with an infrared camera and monitor (DAGE-MTI, Michigan City, IN, USA).

Patch-clamp recording of pyramidal motor cortical neurons Ca^{2+} channel currents

Young (2- to 4-week-old), young adult (7-month-old) and old (28- to 29-month-old) F344XBN rats have been used for patch-clamp recordings. The inclusion of these age groups in the study allows us to differentiate the effects of maturation and senescence on our measurements. Rats were decapitated and the area of brain cortex dissected rapidly and placed in ice-cold saline. Transverse slices (300 μm thick) were prepared using a vibrating slicer (Vibratome Series 10000, TPI, St Louis, MO, USA). Slices were incubated at 32 °C for 30 min and thereafter at room temperature (20–21 °C) until they were transferred to the recording chamber. The volume of the recording chamber was 300 μl. This volume was replaced approximately four times per minute. Brain slices were treated with 0.25 mg pronase E–actinase E enzyme (protease from *Streptomyces griseus*, Sigma) per millilitre of ACSF (see below) for 30 min before recording to get rid of debris and facilitate membrane seal. Pyramidal motor neuron Ca^{2+} channel currents were measured using the whole-cell configuration of the patch-clamp technique (Hamill *et al.* 1981) with an Axopatch 200A amplifier and pClamp 8 software (Axon Instruments, Union City, CA, USA). A Digidata 1200 interface (Axon Instruments) was used for A/D conversion. Patch pipettes were pulled from borosilicate glass (Boralex) using a Flaming Brown micropipette puller (P97; Sutter Instrument Co., Novato, CA, USA) and then fire-polished to obtain electrode resistance ranging from 2 to 4 MΩ when filled with the internal solution. The internal solution contained (mM): 130 CsCl, 20 TEACl, 1 EGTA, 4 MgATP, 0.4 GTP and 10 Hepes (titrated to pH 7.2 with CsOH) (Plant *et al.* 1998). Membrane currents during a voltage pulse, P, were initially corrected by analog subtraction of linear components. The remaining linear components were digitally subtracted on-line using hyperpolarizing control pulses of one-quarter of the test pulse amplitude (−P/4 procedure) as described (Delbono, 1992; Delbono *et al.* 1997). We verified that subpulses elicited no ionic currents. Four control pulses were applied before the test pulse. Potential voltage errors associated with whole-cell recording in large cells were minimized by adequate compensation for whole-cell capacitance transients. The voltage errors were compensated to 70–80 %. Pipette series resistance and linear capacitance of the cell membrane were calculated as described (McCobb *et al.* 1989; Shaefer *et al.* 2003). Cell capacitance was calculated as the integral of the transient current in response to a brief hyperpolarization pulse from −80 (holding potential) to −90 mV. Ca^{2+} channel currents were evoked by depolarizing voltage steps from the holding potential to command potentials ranging from −70 to 50 mV.

The inward Ca^{2+} channel current (I_{Ca})–voltage relationship was fit to the following equation:

$$I_{Ca} = G_{max}(V - V_r)/1 + \exp(z[V_{½} - V]/25.3), \quad (1)$$

where G_{max} is the maximal conductance, V is the membrane potential, V_r is the reversal potential, $V_{½}$ is the half-activation potential, z is the effective valence and 25.3 is the value for RT/F (R is the gas constant, T is the absolute temperature and F is Faraday's constant) at 20 °C.

Solutions and chemicals

The artificial cerebrospinal fluid (ACSF) contained (mM): 124 NaCl, 2.5 KCl, 2 $CaCl_2$, 2 $MgCl_2$, 1.25 NaH_2PO_4, 26 $NaHCO_3$ and 10 dextrose. The pH was equilibrated to 7.3 by gassing the solution with a mixture of 95 % O_2 and 5 % CO_2. To record Ca^{2+} channel currents, the saline solution was replaced with one containing (mM): 105 NaCl, 20 TEACl, 2.5 KCl, 1 $BaCl_2$, 1 $MgCl_2$, 1.25 NaH_2PO_4, 26 $NaHCO_3$, 20 glucose, 0.5 μM tetrodotoxin (TTX), 1 μM strychnine and 10 μM bicuculline (pH 7.3 when gassed with 95 % O_2 and 5 % CO_2) (Plant *et al.* 1998). Ca^{2+} channel currents were blocked using the following toxins: ω-conotoxin (CTx)-

GVIA, ω-agatoxin IVA/ω-conotoxin MVIIC and ω-Aga-IIIA, all purchased to Alomone Labs (Jerusalem, Israel). SNX-482 was purchased to Peptides International (Louisville, KT, USA). Toxins were prepared as stocks in water and kept frozen at −20 °C. Nisoldipine and nifedipine (Sigma, St Louis, MO, USA) stocks solutions were prepared in 100 % ethanol. Toxins were applied using different methods according to specific experiments, as indicated below. The IGF-1R tyrosine kinase inhibitor I-OMe-AG538 (Blum *et al.* 2000; Zheng *et al.* 2002*a*) was purchased to Calbiochem (San Diego, CA, USA). The experiments were carried out at room temperature (20–21 °C).

PCR amplification of the rat brain isoforms RNA encoding the α_1-subunit of the HVA and LVA Ca^{2+} channels

The mRNA encoding the α_1 subunit of the HVA and LVA Ca^{2+} channels expressed in the brain cortex area controlling hindlimb motility was transcribed into cDNA as described (Lambolez *et al.* 1992; Plant *et al.* 1998) with some modifications. RNA was isolated from fresh brain with TRI reagent RNA extraction solution (MRC, OH, USA) as described (Zheng *et al.* 2002*b*). Total RNA preparation was treated with DNase I to get rid of genomic DNA contamination. Reverse transcription was performed in a solution containing 5 μM hexamer random primers (Roche, Indianapolis, IN, USA), 10 mM dithiothreitol, 0.5 mM of four deoxyribonucleotides triphosphate (Pharmacia, Peapack, New Jersey, USA), 20 U of ribonuclease inhibitor (Promega, Madison, WI, USA) and 100 U of Moloney murine leukaemia virus reverse transcriptase (BRL, Gaithersburg, MD, USA). The cDNA encoding HVA and LVA Ca^{2+} channels was amplified using partially degenerate primers that amplified fragments of the rat brain isoforms of the HVA (α_{1A}–α_{1E} and α_{1S}) (Plant *et al.* 1998) and LVA (α_{1G}–α_{1I}) Ca^{2+} channel α_1-subunits. For the detection of $\alpha_{1A–E}$ and α_{1S}, cDNA was digested with the following enzymes *Drd*I, *Bpm*I, *Hinc*II, *Afl*II, *Acc*I and *Cla*I, respectively. Ca^{2+} channels cDNA digestion gave rise to the following fragments 406/184, 268/322, 153/476, 99/542, 178/421 and 413/240 bp corresponding to $\alpha_{1A–E}$ and α_{1S} in agarose gel, according to restriction analysis (Plant *et al.* 1998). The primers for LVA Ca^{2+} channel α_1-subunits were: sense 5′-ATCTTCCTCAACTGTATCACC-3′ and antisense 5′-A(G/T)GTCCAGGTAGTGGCTGGT-3′. The position of the primers on the individual sequences was: sense 3906–3926 and antisense 4842–4861 on α_{1G} (GeneBank access number AF290112, rat brain), sense 3975–3995 and antisense 4890–4909 on α_{1H} (GeneBank AF290213, rat brain) and sense 3421–3441 and antisense 4327–4346 on α_{1I} (GeneBank 290214, rat brain). The sizes of the amplified fragments calculated from the reported sequences were 955, 935 and 926 bp for α_{1G}, α_{1H} and α_{1I}, respectively. A single PCR amplification was performed using FailSafe PCR System kit (Epicentre, Madison, WI, USA). Digestion of LVA Ca^{2+} channels DNA with *Stu*I, *Sac*I or *Cla*I generated two fragments of 794 and 162, 606 and 329, and 706 and 220 bp for α_{1G}, α_{1H} and α_{1I} genes, respectively.

Statistical analysis

Data were analysed using Student's *t* test or analysis of variance (ANOVA). A value of $P < 0.05$ was considered significant. Data are expressed as means ± S.E.M. with the number of observations (n).

RESULTS

Localization of the recording area

Whole-cell patch-clamp recordings were performed on the brain motor cortex involved in controlling the movement of hindlimbs. This area was mapped in a separate group of rats from those used for patch-clamp experiments. Penetration microstimulation mapping confirmed the location and extension of the area described previously (Neafsey *et al.* 1986; Liang *et al.* 1991). The hindlimb motor cortex began at bregma and extended 2–3 mm further caudally. The rostral, caudal, medial and lateral borders of this area were found similar to those described (Neafsey *et al.* 1986).

IGF-1 enhances Ca^{2+} channel currents through HVA Ca^{2+} channels in 2- to 4-week-old rats

Ca^{2+} channel currents carried by Ba^{2+} ions were recorded in pyramidal neurons located on layer V of the brain motor cortex area as described above. Large pyramidal-shaped neurons were identified using an infrared camera and monitor, as described above. To confirm the pyramidal shape of the soma and extension and complexity of the dendrites we filled the neurons with Lucifer yellow via the patch pipette as described (see Methods) in a subset of the cells studied ($n = 15$). Figure 1 illustrates a typical cortical pyramidal motor neuron used for our recordings. The soma and thick apical dendrite (arrow) are the parts of the neuron on focus. Ca^{2+} channel currents were evoked by depolarizing voltage steps from the holding potential (−80 mV) to command potentials ranging from −70 to 50 mV. Brain slices were incubated for 15 min in either IGF-1 (20 ng ml^{-1}) or a combination of the IGF-1R tyrosine kinase inhibitor AG538 (25 μM) (Blum *et al.* 2000) and IGF-1, before recording started. In this case, slices were incubated for 15 min in AG538 followed by 15 min in IGF-1 plus AG538. Figure 2 shows representative Ca^{2+} channel currents from −30 to 30 mV recorded in control (*A*), IGF-1 (*B*) and AG538 plus IGF-1 (*C*). It appears that 20 ng ml^{-1}

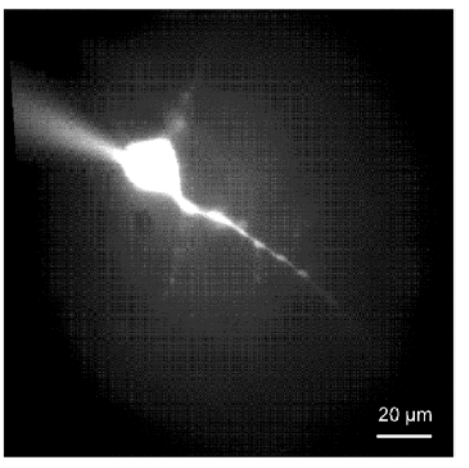

Figure 1. Pyramidal motor neuron from layer V of the rat brain cortex

Digitized image of a pyramidal neuron from layer V of the brain motor cortex filled with Lucifer yellow via the glass electrode used for whole-cell patch-clamp (upper left corner). The cortical motor neuron has a pyramidal-shaped soma with gradually emerging, thick apical dendrite, and basilar dendrites .

IGF-1 significantly enhances HVA Ca^{2+} channel currents, an effect that is prevented by preincubating the brain slice in 25 μM AG538. No interactions between IGF-1 and AG538 were detected other than those reported here and in previous publications (Blum *et al.* 2000, Zheng *et al.* 2002*a*,*b*). Figure 2*D* shows the current–voltage relationship for control (filled circles, 20 cells from 13 rats), IGF-1 (open circles, 17 cells, 11 rats) and AG538 plus IGF-1 (triangles, 15

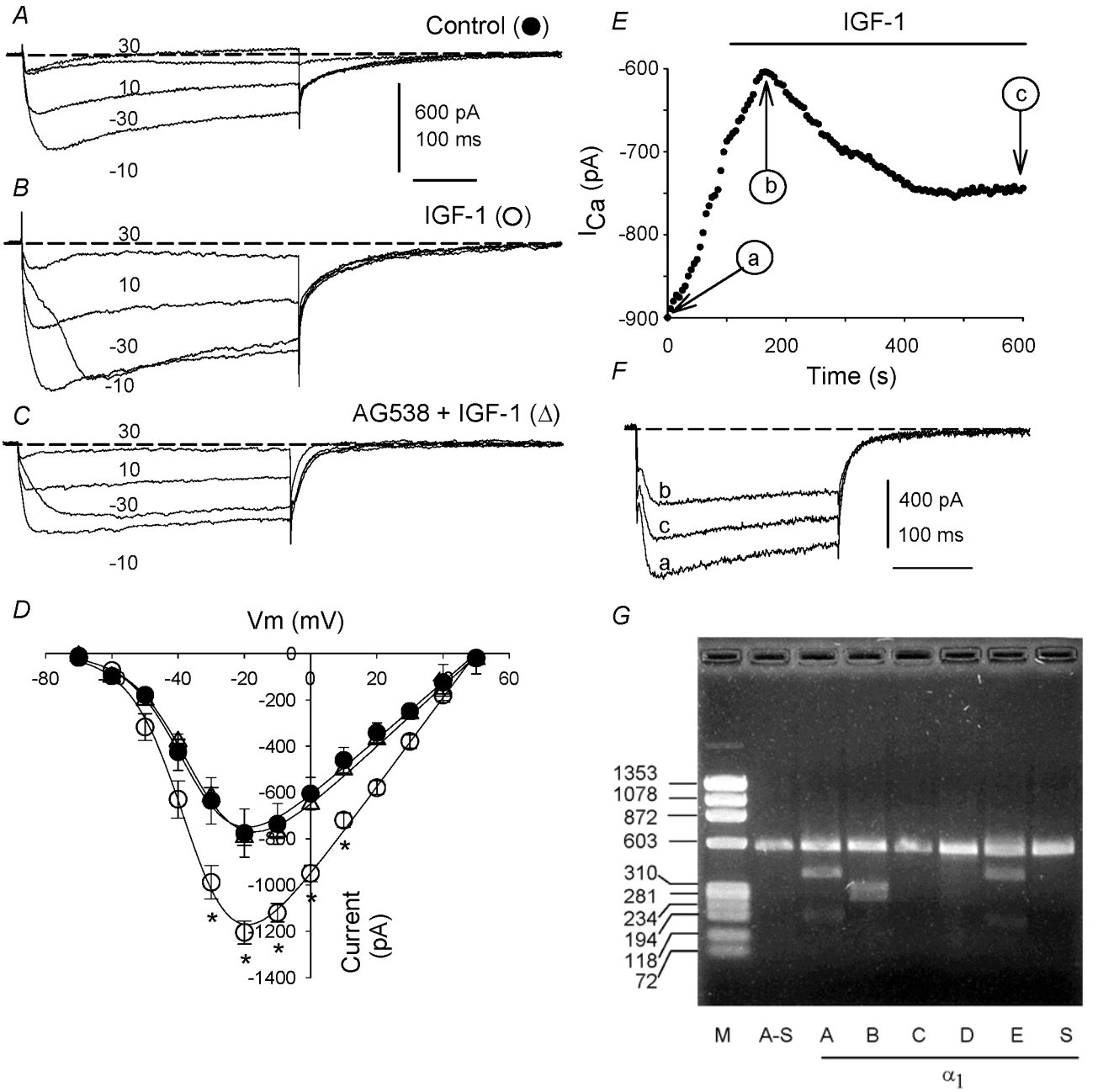

Figure 2. Insulin-like growth factor-1 (IGF-1) enhances Ca^{2+} channel currents through HVA Ca^{2+} channels in 2- to 4-week-old rats

Representative Ca^{2+} channel currents from −30 to 30 mV with 20 mV intervals in control (*A*), IGF-1-treated (*B*) and AG538 plus IGF-1 (*C*). *D*, Ca^{2+} channel current–voltage relationship in control (filled circles), 20 ng ml^{-1} IGF-1 (open circles) and AG538 plus IGF-1 (open triangles). Experimental data were fitted to eqn (1) (see Methods). Asterisks indicate statistically significant differences compared with control ($P < 0.05$). *E*, effect of rapid perfusion of IGF-1 (bar) on high-voltage-activated (HVA) Ca^{2+} channel currents tested in voltage-clamped pyramidal motor neurons pulsed to −10 mV for 250 ms every 5 s. The rate of solution perfusion was 1.0–1.5 ml min^{-1}. *F*, Ca^{2+} channel currents corresponding to control (a), the lowest current amplitude recorded in the cell (b) and IGF-1-dependent potentiation (c) are illustrated. *G*, RT-PCR for HVA Ca^{2+} channel α_1 expression in the brain cortex region used for electrophysiological recordings. M and A-S indicate the lanes in which the marker and undigested Ca^{2+} channel cDNAs, respectively, have been loaded.

Table 1. Average of best-fit parameters describing the voltage dependence of Ca^{2+} channel currents in brain pyramidal motor neurons

Parameters	2- to 4-week-old rat			7-month-old rat		28- to 29-month-old rat	
	Control	IGF-1	AG538 + IGF-1	Control	IGF-1	Control	IGF-1
G_{max} (pS)	12 ± 1	19 ± 2*	13 ± 2	3.3 ± 0.4	7.0 ± 0.9*	4.4 ± 0.5	8.1 ± 0.9*
V_r (mV)	50 ± 7	50 ± 6	51 ± 5	50 ± 3	51 ± 4	52 ± 6	52 ± 4
z	2.9 ± 0.2	3.0 ± 0.2	2.8 ± 0.3	3.0 ± 0.2	3.0 ± 0.4	2.7 ± 0.2	2.9 ± 0.3
$V_{½}$ (mV)	−36 ± 4	−36 ± 3	−34 ± 4	−44 ± 5*	−40 ± 3	−35 ± 3	−37 ± 5

*Statistically significant ($P < 0.05$) differences between IGF-1 treated group and the remaining group(s). G_{max} is the maximal conductance, V is the membrane potential, V_r is the reversal potential, $V_{½}$ is the half-activation potential, z is the effective valence. Values are expressed as means ± S.E.M.

cells, 9 rats). The IGF-1 effect on channel current amplitude was statistically significant from −30 to 10 mV ($P < 0.05$). Data were fitted to eqn (1) and the best-fit parameters are included in Table 1. It is apparent that IGF-1 increases maximal conductance but does not modify the voltage dependence of the Ca^{2+} channel currents. The low-voltage-activated (LVA) Ca^{2+} channel currents did not exhibit statistically significant changes in the amplitude after exposure to IGF-1 (Fig. 2*D*, see also Fig. 6). LVA Ca^{2+} channel currents were inactivated by changing the holding potential from −80 to −60 mV. The effect of IGF-1 on HVA Ca^{2+} channel currents was also tested in voltage-clamped neurons by rapid solution change. The rate of solution change was maintained at 1.0–1.5 ml min^{-1} to avoid stimulation of mechanosensitive N-type Ca^{2+} channels (Calabrese *et al.* 2002). Figure 2*E* illustrates a representative experiment in which a pyramidal motor neuron was pulsed to −10 mV for 250 ms every 5 s, in control conditions and during IGF-1 perfusion (bar). Figure 2*F* shows Ca^{2+} channel current traces corresponding to control (a), the lowest current amplitude recorded in the cell (probably associated with run-down) (b) and IGF-1-dependent potentiation (c) in Fig. 2*E*. The initial fast peak depicted in Fig. 2*F* corresponds to Na^+ currents resistant to 0.5 μM tetrodotoxin. This current was completed blocked by incubation in 5 μM tetrodotoxin (data not shown). A lag of 1–2 min in the appearance of IGF-1-evoked current potentiation is evident. This delay may result from activation of a phosphorylation cascade leading to HVA Ca^{2+} channels phosphorylation (Delbono *et al.* 1997) (see below).

The molecular expression of the HVA Ca^{2+} channels was investigated by RT-PCR in the block of the brain cortex used for electrophysiological recordings (Fig. 2*G*). The α_{1A}, α_{1B} and α_{1E} mRNAs encoding the HVA Ca^{2+} channels P/Q, N and R, respectively, were detected by the presence of the following fragments: 406/184, 322/268 and 421/178, respectively, in agarose gels after enzymatic treatment (Plant *et al.* 1998). Expected fragments for α_{1C} (476/153), α_{1D} (542/99) and α_{1S} (413/240) were not found in any of the five preparations from the five rats studied. These results suggest that IGF-1 enhances Ca^{2+} channel currents through P/Q- and/or N- and/or R-type, but not through L-type Ca^{2+} channels.

To identify the Ca^{2+} channel(s) mediating the IGF-1-induced HVA current potentiation, we blocked the Ba^{2+} conductance through different Ca^{2+} channel subtypes using specific toxins or channel antagonists in acutely perfused brain slices. Figure 3*A* shows the ratio between the peak Ca^{2+} channel currents recorded in the presence and absence of a channel blocker (grey bars), and the ratio between the effect of a Ca^{2+} channel blocker plus IGF-1 and a Ca^{2+} channel blocker alone on the peak Ca^{2+} channel currents (black bar). Ca^{2+} currents were normalized to the extrapolated control value. The dashed lines in Fig. 3*B–H* represent the extrapolation of the Ca^{2+} channel currents recorded during the first 150 s to the end of the experiment. For the statistical analysis, the peak Ca^{2+} channel current before and after the application of a channel blocker or the peak currents recorded in the presence of the channel antagonist and in the presence of the antagonist plus IGF-1, were compared. $P < 0.05$ was considered statistically significant (asterisks). The peak Ca^{2+} channel current was determined by stimulating the cell with command pulses from −70 to 70 mV, with a 10 mV interval. The effects of IGF-1 and/or Ca^{2+} channel toxins were studied on the peak Ca^{2+} current. To this end, the voltage pulse that elicited the maximum current amplitude was applied repetitively afterwards. The exposure time to these compounds is indicated in Fig. 3*B–G* (bars). Figure 3*H* illustrates the time course of the run-down of a control Ca^{2+} channel current. The IGF-1R tyrosine kinase inhibitor AG538 (50 μM) prevented IGF-1-dependent Ca^{2+} channel current potentiation (Fig. 3*A* and *B*). Pre-exposure of the slice to the P/Q-channel toxin ω-Aga-IVA (100 nM) or to the N-type channel toxin ω-CTx-GVIA (2 μM) resulted in partial inhibition of the current (Fig. 3*A*, *C* and *D*) by 20 ± 2.1 and 24 ± 2.7 %, respectively, whereas the combination of these two toxins completely prevented the IGF-1-dependent current potentiation (Fig. 3*A* and *E*). The inhibitor of the R-type Ca^{2+} channel SNX-482 (0.5 μM) did not prevent the IGF-1-evoked potentiation of the Ca^{2+} channel current

Journal of Physiology

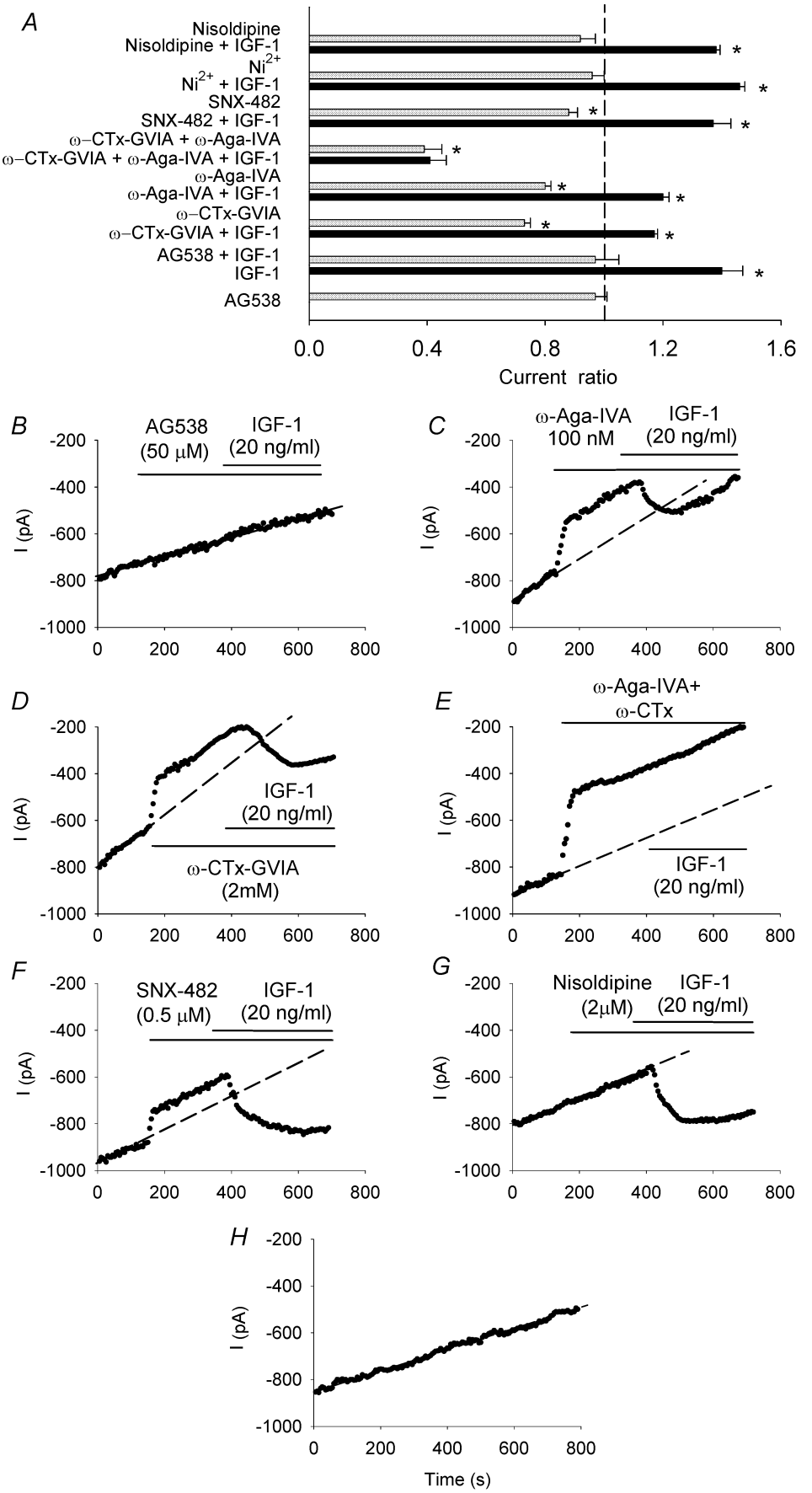

Figure 3. For legend see facing page.

(Fig. 2*A* and *F*). Similarly, the L-type Ca^{2+} channel blockers nisoldipine (2 μM) (Fig. 3*A* and *G*) or nifedipine (2 μM) (data not shown) did not inhibit Ca^{2+} channel current nor prevent IGF-1-dependent current potentiation, consistent with the lack of detectable expression of L-type Ca^{2+} channel in this brain region (Fig. 2*G*). Figure 3*H* illustrates the time course of the Ca^{2+} channel current in the absence of both Ca^{2+} channel toxins and IGF-1. These experiments confirm that IGF-1 potentiation is not related to spontaneous changes in Ca^{2+} current amplitude. The perfusion of the T-channel blocker Ni^{2+} (50 μM) did not prevent IGF-1-dependent current potentiation (Figs 3*A* and 6). These experiments support the conclusion that P/Q- and N-type Ca^{2+} channels mediate the IGF-1-induced enhancement of HVA Ca^{2+} channel currents. To determine whether the IGF-1-dependent potentiation of HVA Ca^{2+} channel currents is preserved at later ages, we investigated the effect of this growth factor on brain slices from young adult and senescent rats.

IGF-1 enhances HVA Ca^{2+} channel currents in young adult rats

Ca^{2+} channel currents recorded in young adult rats (7 months old) had a similar voltage distribution but lower amplitude than that recorded in pyramidal motor neurons from 2- to 4-week-old rats (Fig. 4*A*–*C*). To determine whether the difference in Ca^{2+} channel current amplitude results from changes in pyramidal motor neuron size and/or Ca^{2+} channel density with age, cell capacitance was measured. The mean pyramidal motor neuron capacitance was 14.1 ± 1.9 and 12.2 ± 1.7 pF for 2- to 4-week-old and 7-month-old rats, respectively ($P > 0.05$), supporting the concept that there is no significant changes in cell membrane surface with maturation (see below). Figure 4*C* shows that in young adult rats, similarly to younger animals, IGF-1 (open circles, 18 cells, 14 rats) significantly enhanced Ca^{2+} channel current amplitude compared to control (filled circles, 17 cells, 15 rats) in the −30 to 20 mV voltage range ($P < 0.05$) but did not modify the voltage dependence of the current. The half-activation potential of the current is shifted to more negative potentials compared to the value recorded in 2- to 4-week-old rats (Table 1). The Ca^{2+} channel profile in this brain region demonstrated the expression of α_{1A}, α_{1B} and α_{1E} and the absence of α_{1C}, α_{1D} and α_{1S} (Fig. 4*D*), similar to that described for 2- to 4-week-old rats. The analysis of the Ca^{2+} channels involved in the IGF-1-induced potentiation of the peak Ca^{2+} current (Fig. 4*E*) showed a similar pattern to that described for younger rats (Fig. 3*A*), but the amplitude of the IGF-1 evoked Ca^{2+} current potentiation was more obvious than in younger animals. The magnitude of the current potentiation was 99 and 46 %, respectively.

IGF-1 enhances HVA Ca^{2+} channel currents in senescent rats

Ca^{2+} channel currents recorded in senescent (28–29 month-old) rats (Fig. 5*A* and *B*) have a similar voltage dependence and amplitude to those recorded in neurons from 7-month-old rats, however, the amplitude was significantly lower than in motor neurons from 2- to 4-week-old rats. The mean motor neuron capacitance for 28-month-old rats was 11.8 ± 1.6 pF, a value that is not significantly different to that recorded in 2- to 4-week-old and 7-month-old rats ($P > 0.05$), suggesting that there are not significant changes in cell membrane surface with senescent in this cell population. Preincubation in IGF-1 of the brain slice from 28-month-old rats significantly enhanced Ca^{2+} channel current amplitude in the −30 to 10 mV voltage range and had no effects on the voltage dependence of the currents (Fig. 5*A*–*C* and Table 1). The Ca^{2+} channel expression profile is similar to that described for 2- to 4-week-old and 7-month-old rats. The expression of α_{1A}, α_{1B} and α_{1E} and the absence of α_{1C}, α_{1D} and α_{1S} (Fig. 5*D*) indicates that the pattern of HVA channels expression does not change with senescence in this brain region. The analysis of the Ca^{2+} channels involved in the acute response to IGF-1 (Fig. 5*E*) is similar to that described for young adult rats (Fig. 4*E*) but the magnitude of the peak Ca^{2+} channel current potentiation is more pronounced than that recorded in neurons from 2- to 4-week-old rats (Fig. 3*A*). The IGF-1-dependent current potentiation was 95 and 46 %, respectively, for 28- to 29-month-old and 2- to 4-week-old rats.

IGF-1 does not enhance significantly LVA Ca^{2+} channel currents

The expression of LVA Ca^{2+} channels and their response to the incubation in IGF-1 has been shown above (Figs 2*D*, 4*C* and 5*C*). The effects of acute exposure to the growth factor

Figure 3. Effects of channel blockers on HVA Ca^{2+} channel currents recorded in 2- to 4-week-old rats

A, effects of acute perfusion of a channel blocker alone or in combination with IGF-1 on the peak Ca^{2+} channel current. Bars represent means ± S.E.M. of the ratio between the peak Ca^{2+} channel current recorded in the presence and absence of a channel blocker (grey bars) and the ratio between the effect of the combination of a Ca^{2+} channel blocker plus IGF-1 and a Ca^{2+} channel blocker alone on the peak Ca^{2+} channel current (black bars). Asterisks indicate the statistical significance ($P < 0.05$). *B*–*G*, representative experiments included in *A*. *H*, time course of the run-down of a control Ca^{2+} channel current. Dashed lines represent the extrapolation of the current run-down (see text). Bars on top of each graph indicate the exposure time to a drug and/or IGF-1.

were studied in a separate group of experiments. Figure 6*A* shows that the rat brain T-type Ca^{2+} channel family (α_{1G}, α_{1H} and α_{1I}) is expressed throughout the lifespan in the motor cortex involved in hindlimb motility. Although these results do not necessarily indicate that pyramidal motor neurons express T-type channels, the three channel subtypes have been detected by *in situ* hybridization in layer V of the cerebral cortex (Talley *et al.* 1999). The T-type α_{1I} isoform predominates in the three age groups, showing cDNA fragments in agarose gel at 706 and 220 bp after enzymatic digestion. Considerably lower amounts of the T-type channels α_{1G} and α_{1H} were detected in the three age groups in five preparations from five rats. The cDNA fragments corresponding to α_{1G} and α_{1H} are 794/162 and 606/329 bp, respectively. Figure 6*B* illustrates an experiment in which a brain slice was acutely exposed to IGF-1 for the time indicated (bar). Pyramidal motor neurons from 2- to 4-week-old rats were voltage-clamped at a holding potential of −80 mV and pulsed to a command voltage of −50 mV. Figure 6*C* illustrates the first (a) and last (b) currents plotted in Fig. 6*B*. It appears that IGF-1 did not enhance the current amplitude. No potentiation was recorded in any of the cells

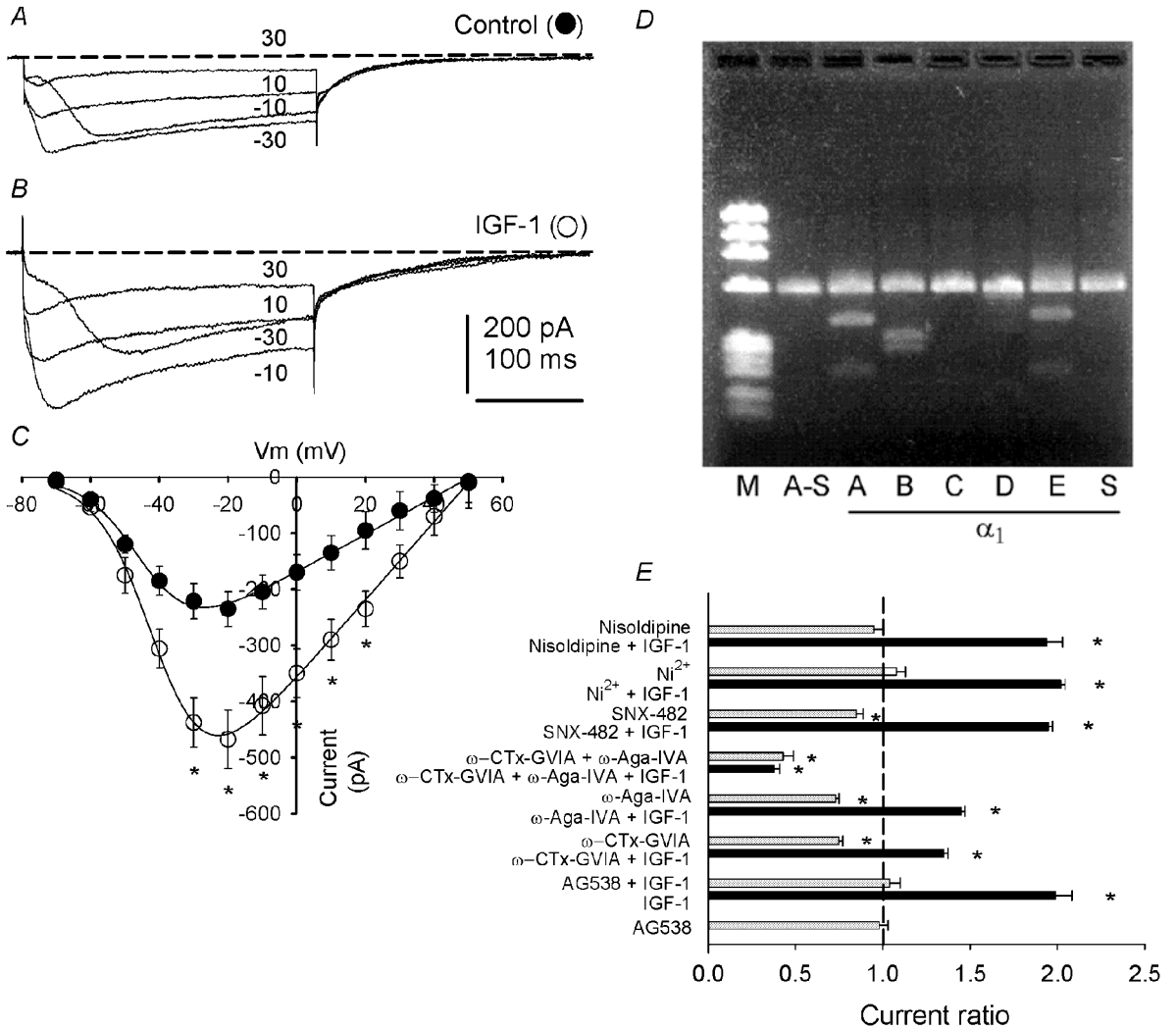

Figure 4. IGF-1 enhances HVA Ca^{2+} channel currents in young adult rats

Representative Ca^{2+} channel current records from −30 to 30 mV with 20 mV intervals in control (*A*) and IGF-1-treated (*B*) pyramidal motor neurons. *C*, Ca^{2+} channel current–voltage relationship in control (filled circles) and after treatment with 20 ng ml^{-1} IGF-1 (open circles). Experimental data were fitted to eqn (1). Average best-fit parameters are shown in Table 1. Asterisks indicate statistically significant difference ($P < 0.05$). *D*, RT-PCR for HVA Ca^{2+} channel α_1 expression in brain motor cortex. M and A-S indicate the lanes in which the marker and undigested Ca^{2+} channel cDNAs, respectively, were loaded. *E*, effects of acute perfusion of a channel blocker alone or in combination with IGF-1 on the peak Ca^{2+} channel current. Bars represent means ± S.E.M. of the ratio between the peak Ca^{2+} channel current recorded in the presence and absence of a channel blocker (grey bars) and the ratio between the effect of the combination of a Ca^{2+} channel blocker plus IGF-1 and a Ca^{2+} channel blocker alone on the peak Ca^{2+} channel current (black bar). Asterisks indicate the statistical significance ($P < 0.05$).

tested (n = 11 slices from four rats). Changes in the holding potential (to −90 or −110 mV) or command pulse (at −60, −40 mV) did modify the effect of IGF-1 on the peak Ca^{2+} channel current. No potentiation was observed in either slices from young adult (n = 7 slices from four rats) or from senescent (10 slices from five rats) rats (data not shown).

DISCUSSION

To design rational interventions to prevent and/or delay functional impairment of movement control, it is crucial to determine whether central nervous system neurons remain responsive to growth factors at later stages of life. IGF-1 is a key factor involved in maintenance of brain structure and function throughout life based on its role in neuronal differentiation and maturation (Arsenijevic & Weiss 1998; Ye *et al.* 2002), ion channel function and cell excitability (see above). Here, we show that HVA Ca^{2+} channels expressed in pyramidal motor neurons of layer V of the brain motor cortex from 2- to 4-week-old rats are responsive to IGF-1 and retain this capacity during maturation and senescence.

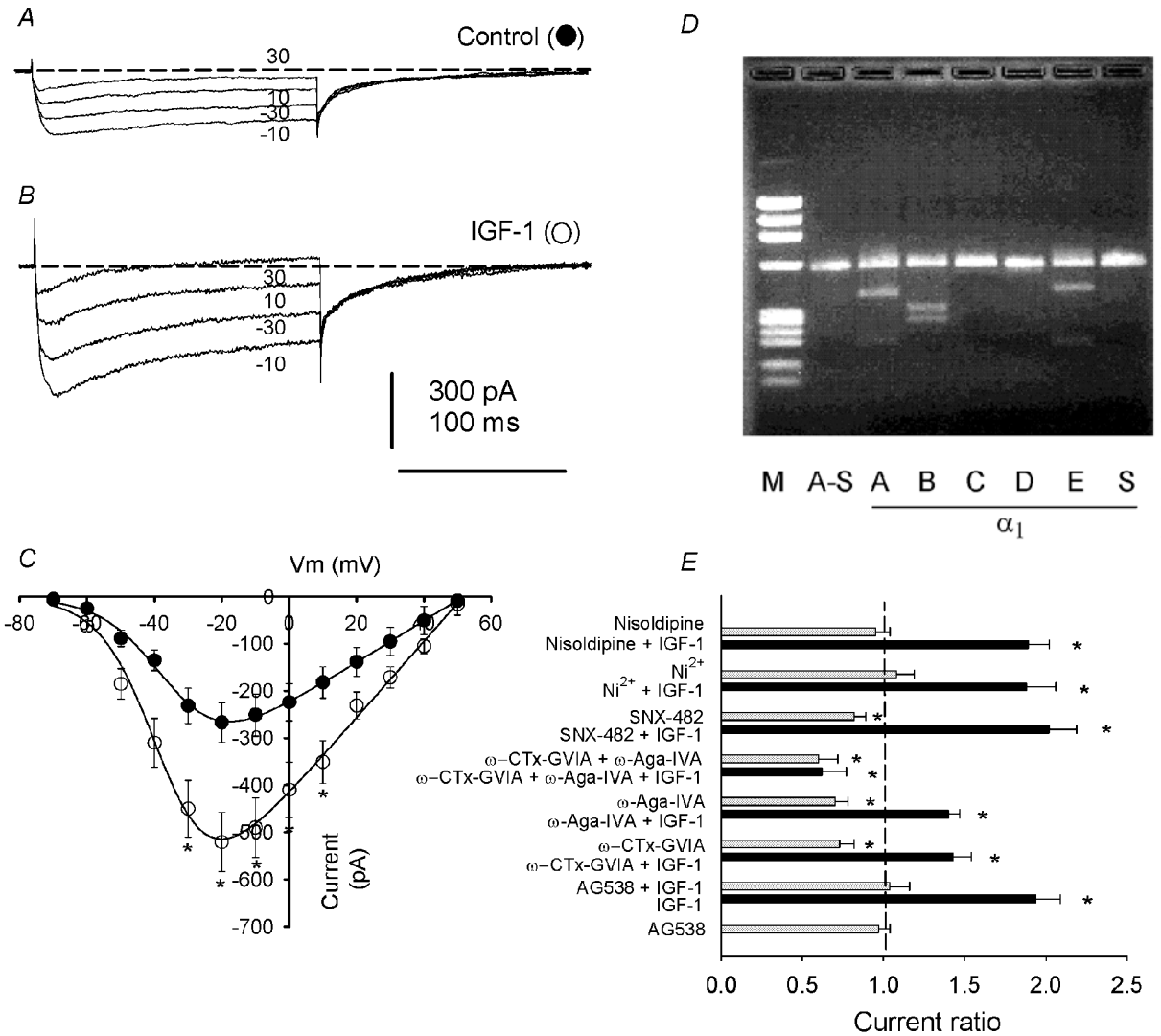

Figure 5. IGF-1 enhances HVA Ca^{2+} channel currents in senescent rats

Representative Ca^{2+} channel current records from −30 to 30 mV with 20 mV intervals in control (*A*) and IGF-1-treated (*B*) pyramidal motor neurons from 28-month-old rats. *C*, IGF-1 significantly enhanced Ca^{2+} channel current amplitude in the −30 to 20 mV voltage range and no effects on the current–voltage relationship was observed. The average best-fit parameters are shown in Table 1. *D*, agarose gel showing the expression of α_{1A}, α_{1B} and α_{1E} and absence of α_{1C}, α_{1D} and α_{1S} in brain motor cortex. *E*, effects of acute perfusion of a channel blocker alone or in combination with IGF-1 on the peak Ca^{2+} channel currents. Bars represent means ± S.E.M. of the ratio between the peak Ca^{2+} channel currents recorded in the presence and absence of a channel blocker (grey bars) and the ratio between the effect of the combination of a Ca^{2+} channel blocker plus IGF-1 and a Ca^{2+} channel blocker alone on the peak Ca^{2+} channel currents (black bar). Asterisks indicate the statistical significance.

Decline of motor control in senescent mammals

The paucity of data involving the cortical pyramidal motor neuron is in contrast with the substantial evidence for alterations in the structure and function of the nerve and muscle in the decline in strength and mobility of the elderly (for a review see Delbono, 2003). Technical difficulties in assessing function have probably hindered a more comprehensive understanding of the role of the central nervous system in the age-dependent decline in motor function. Slowing of movements and loss of fine motor skills in human ageing are thought to reflect alterations in brain systems subserving motor function (Smith *et al.* 1999). It has been reported that elderly subjects show decreased activation of task-specific canonical areas in comparison with young subjects (Mattay *et al.* 2002). Elderly subjects demonstrated greater activation in both spatial extent and magnitude in not only the contralateral primary motor cortex, an area critical for motor execution, but in other cortical and subcortical regions involved in motor processing, and also in ipsilateral areas (Mattay *et al.* 2002). A steep decline in motor performance (Smith *et al.* 1999) coincides approximately with the reported decrease in peripheral motor function in individuals after age 60 years (Hurley, 1995).

Ca^{2+} channels type expression in pyramidal neurons of the brain motor cortex

It is known that the level of expression of the Ca^{2+} channel subtypes in the central nervous system varies according to the region explored (Mynlieff & Beam, 1992; Randall & Tsien, 1995; Umemiya & Berger, 1995), but information about the Ca^{2+} channel population in pyramidal neurons from layer V of the brain cortex involved in hindlimb control is not available. In the present study, we report that pyramidal motor neurons from this area express HVA Ca^{2+} channels. N-, P/Q- and R-type Ca^{2+} channels, encoded by α_{1B}, α_{1A} and α_{1E} genes, respectively, contribute to the recorded HVA whole-cell currents. The expression of N- and P/Q-channels in this region is consistent with previous studies in neocortical pyramidal neurons (Pineda *et al.*

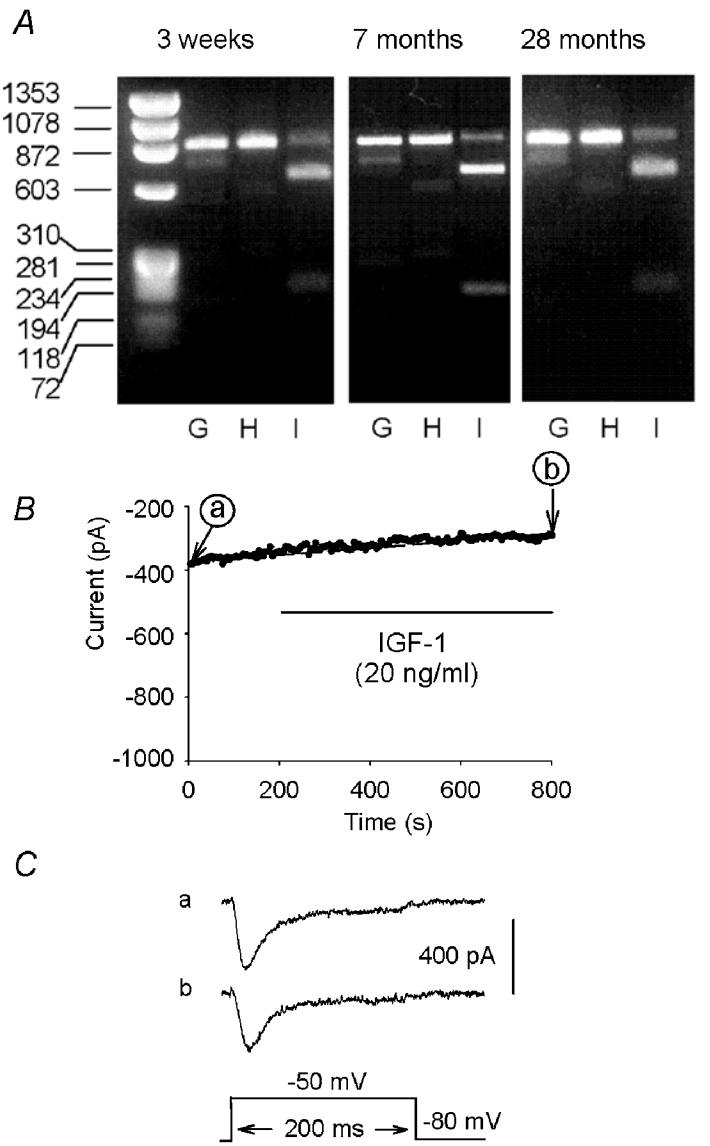

Figure 6. Effects of IGF-1 on LVA Ca^{2+}channel currents

A, agarose gel showing LVA Ca^{2+} channel expression in brain motor cortex from young (3-week-old), young adult (7-month-old) and senescent (28-month-old) rats. *G–I*, indicate the three T-type Ca^{2+} channel isoforms. The first lane on the left shows the marker. *B*, peak channel current amplitude–time relationship. Pyramidal motor neuron from a 3-week-old rat, voltage-clamped at a holding potential of −80 mV and pulsed to a command voltage of −50 mV for 250 ms every 5 s. The bar corresponds to the time the cell was exposed to IGF-1. *C*, illustration of the current traces corresponding to the first (a) and last (b) pulse in *B*.

1998). The use of the tarantula venom SNX-482 allowed us to characterize the expression of R-type Ca^{2+} channels. L-type Ca^{2+} channels have been reported in acutely dissociated pyramidal neurons from sensorimotor cortex (Lorenzon & Foehring, 1995*a*); however, they have not been found in the RT-PCR analysis of brain and brain stem motor nuclei (Plant *et al.* 1998). These results are consistent with the lack of pharmacological and molecular evidence for L-type Ca^{2+} channel expression in our preparation.

Ca^{2+} channel currents recorded in the present study represent a fraction of the Ca^{2+} channels expressed in the cortical motor neurons because they are missing those expressed in distal dendritic compartments. It is not known whether qualitative or quantitative differences exist in the population of Ca^{2+} channels expressed in the soma and proximal dendrites compared to distal dendrites of brain cortex pyramidal motor neurons. Electrophysiological recordings in acutely dissociated brain cortex pyramidal neurons suggest a differential expression of voltage-gated Ca^{2+} channels (Lorenzon & Foehring, 1995*a*,*b*). The expression of T-, N-, L- and R-type Ca^{2+} channels in the soma and P-type channels in distal axons of facial motor neurons has been reported (Plant *et al.* 1998). Immunostaining procedures in rat spinal cord motor neurons showed expression of P/Q-type Ca^{2+} channels in nerve terminals located along the cell bodies and dendrites, N-type Ca^{2+} channels along the cell surface membrane and nerve terminals, and L-type Ca^{2+} channels in the soma and proximal dendrites (Westenbroek *et al.* 1998).

We have found that the maximal conductance of HVA channels decreased from 2- to 4-week-old to 7-month-old rats, whereas no significant difference was detected between young adult and senescent rats. The decline in the peak Ca^{2+} channel conductance with maturation occurs in the absence of significant changes in membrane capacitance, which suggests that Ca^{2+} channel density and/or regulation changes across ages. The lack of changes in membrane capacitance reported here is consistent with previous reports on hippocampal CA1 pyramidal neurons from 2- to 3-month-old rabbits and those older than 36 months (Power *et al.* 2002) and neocortical neurons from neonatal to 4- to 5-week-old rats (Lorenzon & Foehring, 1995*b*). The HVA current density and current–voltage relationship were reported unchanged in Fisher 344 rats aged from 1 to 26.5 months in acutely dissociated basal forebrain neurons (Murchison & Griffith, 1996). However, an increase in Ca^{2+} current density from neonatal to adult followed by a decline in senescent rats has been described in dorsal root ganglion neurons (Kostyuk *et al.* 1993). Studies on the expression, modulation and properties of HVA Ca^{2+} channel function with ageing are needed to fully address differences in Ca^{2+} channel conductance with ageing among different brain regions.

Ca^{2+} channel conductances of 7, 14, 20 and 28 pS have been reported in rat hypoglossal motor neurons using 110 mM Ba^{2+} as a charge carrier (Umemiya & Berger, 1995). These conductance values correspond to T-, N-, P- and L-type Ca^{2+} channels, respectively. The absence of L-type Ca^{2+} channel expression in our preparation together with a considerably lower Ba^{2+} concentration in the bathing solution account for the lower maximal conductance recorded. Although RT-PCR experiments did not allow us to locate the specific cell population expressing the Ca^{2+} channel subtypes mentioned above, they confirmed electrophysiological data on the channels that do not express in pyramidal motor neurons.

Although the population of pyramidal motor neurons studied here is mainly involved in the control of hindlimb motility, this is probably a heterogeneous group of cells. The percentage contribution of each Ca^{2+} channel population to the whole-cell Ca^{2+} channel current varies from neuron to neuron (Lorenzon & Foehring, 1995*a*; Plant *et al.* 1998). Also, probably not all of the pyramidal motor neurons recorded project to the spinal cord, other projections are corticostriatal, corticotectal, corpus callosum, etc. and probably the population of Ca^{2+} channels varies from one to another pyramidal cell (Stewart & Foehring, 2000). The heterogeneity in motor neuron projections and Ca^{2+} channel expression can contribute to their firing pattern (Connors & Gutnick, 1990; Chagnac-Amitai *et al.* 1990) and to their ultimate functional role in motility control.

The three subtypes of T-channels (α_{1G}, α_{1H} and α_{1I}) that contribute to neuronal excitability (Chemin *et al.* 2002) have been found in the region of the brain cortex explored in the present study. Meanwhile α_{1G} is expressed predominantly in cerebellum, hippocampus, thalamus and olfactory bulb (Klugbauer *et al.* 1999). It has been reported that α_{1G} and α_{1H} mRNAs are expressed in various regions of the adult rat brain, while α_{1I} mRNA is restricted to the striatum (McRory *et al.* 2001). In contrast, a more diffuse expression of α_{1I}, including brain cortex, has been described by other groups (Talley *et al.* 1999). As a non-significant trend of IGF-1 to enhance Ca^{2+} channel current amplitude in the low-voltage range (−70 to −40 mV) has been detected, no further characterization of the contribution of any of the three channel subtypes to the whole-cell current was carried out. An explanation for the differential effect of IGF-1 on HVA and LVA Ca^{2+} channels in the pyramidal motor neurons is not obvious.

Mechanism of action of IGF-1 on voltage-activated Ca^{2+} channels

Most of our current knowledge on IGF-1-evoked regulation of VGCC derives from studies in skeletal muscle cells in which IGF-1 enhances L-type Ca^{2+} channel expression by regulating gene transcription (Zheng *et al.* 2002*a*,*b*). In addition, IGF-1 modulates channel function by activating

a protein kinase cascade that results in channel phosphorylation (Kleppisch *et al.* 1992; Delbono *et al.* 1997). IGF-1 also enhances Ca^{2+} channel currents through L- and N-type Ca^{2+} channels in clonal GH4C1 pituitary cells and cultured cerebellar neurons from postnatal day (P)5–P7 rats (Selinfreund & Blair, 1994; Blair & Marshall, 1997). The enhancement of Ca^{2+} entry through VGCC has been reported to fail in muscle cells from ageing rodents, a phenomenon that can be explained by alterations in channel phosphorylation (Delbono *et al.* 1997).

N-, P/Q- and R-type Ca^{2+} channels mediate the IGF-1-induced enhancement of HVA Ca^{2+} channel currents. IGF-1 interaction with IGF-1R might result in HVA Ca^{2+} channel phosphorylation by activating a signalling cascade involving tyrosine kinase and probably other protein kinase(s), as demonstrated for the L-type Ca^{2+} channel α_1 subunit expressed in skeletal muscle fibres from the adult mouse (Delbono *et al.* 1997). The prevention of Ca^{2+} current potentiation by tyrosine kinase inhibitors, together with the involvement of protein kinase C (PKC) in L-type Ca^{2+} channel phosphorylation (Delbono *et al.* 1997), support the concept that the activation of a phosphorylation cascade may modulate HVA Ca^{2+} channels conductance in cortical motor neurons.

It can be postulated that despite the decrease in circulating levels of liver IGF-1, autocrine and paracrine effects of IGF-1 on the brain, resulting from local production by neurons, meninges and blood vessels, are maintained in senescent rodents (Lund *et al.* 1986; Niblock *et al.* 1998; Sonntag *et al.* 1999). However, a significant decrease in IGF-1 and IGF-1R proteins in rat brain between 11 and 32 months of age in cortical layer V has been reported (Sonntag *et al.* 1999). A role for local, in contrast to systemic IGF-1, in the preservation of brain function finds support in the lack of correlation between the plasma levels of IGF-1 and Ca^{2+} channel function. We report here a decrease in the Ca^{2+} channel current amplitude with maturation but not with senescence, whereas the plasma IGF-1 declines from adulthood to senescence. D'Acosta *et al.* (1993) have reported mean plasma concentrations of IGF-1 (in nanograms per millilitre) of 114 and 97 in 10- and 29-month-old rats, respectively. Shimokawa *et al.* (2002) reported an IGF-1 plasma concentration of 157.3 ± 55 ng ml^{-1} for 6-month-old rats. The plasma IGF-1 concentrations reported by Velasco and collaborators (2001) (mean values) were 82 and 47 % for 11- and 27-month-old rats compared with 3-month-old rats, respectively.

The magnitude of Ca^{2+} channel current potentiation evoked by IGF-1 is more obvious in young adults (99 %) and senescent (95 %) than in 2- to 4-week-old rats (46 %). We speculate that this could be an indication that basal HVA Ca^{2+} channel phosphorylation is higher, and consequently further phosphorylation is limited in very young rodents. The reduction or suppression of IGF-1-dependent transcriptional activity over a prolonged period in brain might have multiple effects in addition to L-type Ca^{2+} channel expression. Whether IGF-1 activates a tyrosine kinase–PKC cascade as postulated for skeletal muscle (Delbono *et al.* 1997), an Akt-PI-3 kinase signalling, as postulated for cerebellar granule neurons (Blair *et al.* 1999) or some other mechanism leading to phosphorylation of HVA Ca^{2+} channels in brain cortex layer V pyramidal motor neurons, is not known at the present time.

The levels of and interaction with insulin-like growth factor binding proteins (IGFBPs) determines the bioavailability and activity of IGF-1. The relation between IGF-1 and IGF-1 binding proteins is very complex on various tissues. IGFBP2 inhibits IGF-1, both *in vivo* and *in vitro* (Jones & Clemmons 1995; Clemmons *et al.* 1995). IGFBP5 and IGFBP6 are IGF-1 inhibitors (Babajko *et al.* 1997; D'Acosta *et al.* 1998). Upregulation of IGFBP-2, -5 and/or -6 might prevent binding of IGF-1 to IGF-1R leading to a compensatory increase in IGF-1R. However, this mechanism can be argued based on the reported decrease in IGF-1R in cortical layer V with age (Sonntag *et al.* 1999). Local isoforms of IGF-1 seem to play a major role in tissue trophism, function, maintenance and repair (Hill & Goldspink, 2003). It has been shown that IGF-1 is differentially spliced in response to local demands in skeletal muscle (Hill & Goldspink, 2003); however, this is not known in brain. It seems that the large molecular weight IGF-1 mRNAs predominate in brain, and although not tested, post-transcriptional regulation of IGF-1 synthesis may be particularly relevant in this tissue (Lund, 1994).

Changes in the neuroendocrine system have been postulated as a mechanism of ageing together with cellular and intercellular stochastic theories (for a review see Holliday, 1996; Arking, 1998). IGF-1 signalling plays a role in both life span and tissue structure and function (Wolkow *et al.* 2000). IGF-1 has several targets and is involved in a number of neuronal functions (see above). Considerable evidence support the tenet that changes in the neuroendocrine system may result in age-related changes in organ function (for a review see Delbono, 2003). The age-related decline in pulsatile secretion of growth hormone leads to significant decrease in circulating IGF-1 with potential impact on those targets. Therefore, the preservation of pyramidal neuron responsiveness to IGF-1 throughout life substantiates a role for its use in intervention of the age-related decline in brain motor function.

REFERENCES

Aberg MA, Aberg ND, Hedbacker H, Oscarsson J & Eriksson PS (2000). Peripheral infusion of IGF-I selectively induces neurogenesis in the adult rat hippocampus. *J Neurosci* **20**, 2896–2903.

Arking R (1998). *Biology of Aging: Observations and Principles*. Sinauer Associates, Inc., Sunderland, Massachusetts.

Arsenijevic Y & Weiss S (1998). Insulin-like growth factor-I is a differentiation factor for postmitotic CNS stem cell-derived neuronal precursors: distinct actions from those of brain-derived neurotrophic factor. *J Neurosci* **18**, 2118–2128.

Babajko S, Leneuve P, Loret C & Binoux M (1997). IGF-binding protein-6 is involved in growth inhibition in SH-SY5Y human neuroblastoma cells: its production is both IGF- and cell density-dependent. *J Endocrinol* **152**, 221–227.

Berridge MJ, Lipp P & Bootman MD (2000). The versatility and universality of calcium signalling. *Nature Rev* **1**, 11–21.

Blair LA, Bence-Hanulec KK, Mehta S, Franke T, Kaplan D & Marshall J (1999). Akt-dependent potentiation of L channels by insulin-like growth factor-1 is required for neuronal survival. *J Neurosci* **19**, 1940–1951.

Blair LAC & Marshall J (1997). IGF-1 modulates N and L calcium channels in a PI 3-kinase-dependent manner. *Neuron* **19**, 421–429.

Blum G, Gazit A & Levitzki A (2000). Substrate competitive inhibitors of IGF-1 receptor kiinase. *Biochem* **39**, 15705–15712.

Bondy C, Werner H, Roberts CT Jr & Leroith D (1992). Cellular pattern of type-I insulin-like growth factor receptor gene expression during maturation of the rat brain: comparison with insulin-like growth factors I and II. *Neurosci* **46**, 909–923.

Brooker GJ, Kalloniatis M, Russo VC, Murphy M, Werther GA & Bartlett PF (2000). Endogenous IGF-1 regulates the neuronal differentiation of adult stem cells. *J Neurosci Res* **59**, 332–341.

Calabrese B, Tabarean IV, Juranka P & Morris CE (2002). Mechanosensitivity of N-type calcium channel currents. *Biophys J* **83**, 2560–2574.

Chagnac-Amitai Y, Luhmann HJ & Prince DA (1990). Burst generating and regular spiking layer 5 pyramidal neurons of rat neocortex have different morphological features. *J Comp Neurol* **296**, 598–613.

Chemin J, Monteil A, Perez-Reyes E, Bourinet E, Nargeot J & Lory P (2002). Specific contribution of human T-type calcium channel isotypes (alpha(1G), alpha(1H) and alpha(1I)) to neuronal excitability. *J Physiol* **540**, 3–14.

Chrysis D, Calikoglu AS, Ye P & D'Ercole AJ (2001). Insulin-like growth factor-I overexpression attenuates cerebellar apoptosis by altering the expression of Bcl family proteins in a developmentally specific manner. *J Neurosci* **21**, 1481–1489.

Clemmons DR, Busby WH, Arai T, Nam TJ, Clarke JB, Jones JI & Ankrapp DK (1995). Role of insulin-like growth factor binding proteins in the control of IGF actions. *Prog Growth Factor Res* **6**, 357–366.

Connors BW & Gutnick MJ (1990). Intrinsic firing patterns of diverse neocortical neurons. *Trends Neurosci* **13**, 99–104.

D'Costa AP, Lenham JE, Ingram RL & Sonntag WE. (1993). Moderate caloric restriction increases type 1 IGF receptors and protein synthesis in aging rats. *Mech Ageing Dev* **71**, 59–71.

D'Costa AP, Prevette DM, Houenou LJ, Wang S, Zackenfels K, Rohrer H, Zapf J, Caroni P & Oppenheim RW (1998). Mechanisms of insulin-like growth factor regulation of programmed cell death of developing avian motoneurons. *J Neurobiol* **39**, 379–374.

Delbono O (1992). Calcium current activation and charge movement in denervated mammalian skeletal muscle fibres. *J Physiol* **451**, 187–203.

Delbono O (2003). Neural control of aging skeletal muscle. *Aging Cell* **2**, 21–29.

Delbono O, Renganathan M & Messi ML (1997). Regulation of mouse skeletal muscle L-type Ca^{2+} channel by activation of the insulin-like growth factor-1 receptor. *J Neurosci* **17**, 6918–6928.

Florini JR, Ewton DZ & Coolican SA (1996). Growth hormone and insulin growth factor system in myogenesis. *Endocr Rev* **17**, 481–517.

Georgopoulos AP, Kalaska JF, Caminiti R & Massey JT (1982). On the relations between the direction of two-dimensional arm movements and cell discharge in primate motor cortex. *J Neurosci* **2**, 1527–1537.

Hamill OP, Marty A, Neher E, Sakmann B & Sigworth FJ (1981). Improved patch-clamp techniques for high-resolution current recording from cells and cell-free patches. *Pflugers Arch* **391**, 85–100.

Hill M & Goldspink G (2003). Expression and splicing of the insulin-like growth factor gene in rodent muscle is associated with muscle satellite (stem) cell activation following local tissue damage. *J Physiol* **549**, 409–418.

Ho KY, Evans WS, Blizzard RM, Veldhuis JD, Merriam GR, Samojlik E, Furlanetto R, Rogol AD, Kaiser DL & Thorner MO (1987). Effects of sex and age on the 24-hour profile of growth hormone secretion in man: importance of endogenous estradiol concentrations. *J Clin Endocrinol Metab* **64**, 51–58.

Holdefer RN & Miller LE (2002). Primary motor cortical neurons encode functional muscle synergies. *Exp Brain Res* **146**, 233–243.

Holliday R (1996). Understanding ageing. Cambridge University Press, New York.

Hurley BF (1995). Age, gender, and muscular strength. *J Gerontol A Biol Sci Med Sci* **50**, 41–44.

Jones JI & Clemmons DR (1995). Insulin-like growth factors and their binding proteins: biological actions. *Endocr Rev* **16**, 3–34.

Kleppisch T, Klinz F-Z & Hescheler J (1992). Insulin-like growth factor I modulates voltage-dependent Ca^{2+} channels in neuronal cells. *Brain Res* **591**, 283–288.

Klugbauer N, Marais E, Lacinova L & Hofmann F (1999). A T-type calcium channel from mouse brain. *Pflugers Arch* **437**, 710–715.

Kostyuk P, Pronchuk N, Savchenko A & Verkhratsky A (1993). Calcium currents in aged rat dorsal root ganglion neurones. *J Physiol* **461**, 467–483.

Krampe RT (2002). Aging, expertise and fine motor movement. *Neurosci Biobehav Rev* **26**, 769–776.

Lambolez B, Audinat E, Bochet P, Crepel F & Rossier J (1992). AMPA receptor subunits expressed by single Purkinje cells. *Neuron* **9**, 247–258.

Leonard CT, Matsumoto T, Diedrich PM & McMillan JA (1997). Changes in neural modulation and motor control during voluntary movement of older individuals. *J Gerontol A Biol Sci Med Sci* **52**, M320–325.

Liang FY, Moret V, Wiesendanger M & Rouiller EM (1991). Corticomotoneuronal connections in the rat: evidence from double-labeling of motoneurons and corticospinal axon arborizations. *J Comp Neurol* **311**, 356–366.

Lorenzon NM & Foehring RC (1995*a*). Characterization of pharmacologically identified voltage-gated calcium channel currents in acutely isolated rat neocortical neurons. I. Adult neurons. *J Neurophysiol* **73**, 1430–1442.

Lorenzon NM & Foehring RC (1995*b*). Characterization of pharmacologically identified voltage-gated calcium channel currents in acutely isolated rat neocortical neurons. II. Postnatal development. *J Neurophysiol* **73**, 1443–1451.

Lund PK (1994). Insulin-like growth factor I: molecular biology and relevance to tissue-specific expression and action. *Recent Prog Horm Res* **49**, 125–148.

Lund PK, Moats-Staats BM, Hynes MA, Simmons JG, Jansen M, D'Ercole AJ & Van Wyk JJ (1986). Somatomedin-C/insulin-like growth factor-I and insulin-like growth factor-II mRNAs in rat fetal and adult tissues. *J Biol Chem* **261**, 14539–14544.

McCobb DP, Best PM, & Beam KG (1989). Development alters the expression of calcium currents in chick limb motoneurons. *Neuron* **2**, 1633–1643.

McRory JE, Santi CM, Hamming KS, Mezeyova J, Sutton KG, Baillie DL, Stea A & Snutch TP (2001). Molecular and functional characterization of a family of rat brain T-type calcium channels. *J Biol Chem* **276**, 3999–4011.

Marks JL, Porte D Jr & Baskin DG (1991). Localization of type I insulin-like growth factor receptor messenger RNA in the adult rat brain by in situ hybridization. *Mol Endocrinol* **5**, 1158–1168.

Mattay VS, Fera F, Tessitore A, Hariri AR, Das S, Callicott JH & Weinberger DR (2002). Neurophysiological correlates of age-related changes in human motor function. *Neurology* **58**, 630–635.

Murchison D & Griffith WH (1996). High-voltage-activated calcium currents in basal forebrain neurons during aging. *J Neurophysiol* **76**, 158–174.

Mynlieff M & Beam KG (1992). Characterization of voltage-dependent calcium currents in mouse motoneurons. *J Neurophysiol* **68**, 85–92.

Neafsey EJ, Bold EL, Haas G, Hurley-Gius KM, Quirk G, Sievert CF & Terreberry RR (1986). The organization of the rat motor cortex: a microstimulation mapping study. *Brain Res* **396**, 77–96.

Niblock MM, Brunso-Bechtold JK, Lynch CD, Ingram RL, McShane T & Sonntag WE (1998). Distribution and levels of insulin-like growth factor I mRNA across the life span in the Brown Norway × Fischer 344 rat brain. *Brain Res* **804**, 79–86.

Niblock MM, Brunso-Bechtold JK & Riddle DR (2000). Insulin-like growth factor I stimulates dendritic growth in primary somatosensory cortex. *J Neurosci* **20**, 4165–4176.

Niikura T, Hashimoto Y, Okamoto T, Abe Y, Yasukawa T, Kawasumi M, Hiraki T, Kita Y, Terashita K, Kouyama K & Nishimoto I (2001). Insulin-like growth factor I (IGF-I) protects cells from apoptosis by Alzheimer's V642I mutant amyloid precursor protein through IGF-I receptor in an IGF-binding protein-sensitive manner. *J Neurosci* **21**, 1902–1910.

Pineda JC, Waters RS & Foehring RC (1998). Specificity in the interaction of HVA Ca^{2+} channel types with Ca^{2+}-dependent AHPs and firing behavior in neocortical pyramidal neurons. *J Neurophysiol* **79**, 2522–2534.

Plant TD, Schirra C, Katz E, Uchitel O & Konnerth A (1998). Single-cell RT-PCR and functional characterization of Ca^{2+} channels in motoneurons of the rat facial nucleus. *J Neurosci* **18**, 9573–9584.

Power JM, Wu WW, Sametsky E, Oh MM & Disterhoft JF (2002). Age-related enhancement of the slow outward calcium-activated potassium current in hippocampal CA1 pyramidal neurons *in vitro*. *J Neurosci* **22**, 7234–7243.

Randall A & Tsien RW (1995). Pharmacological dissection of multiple types of Ca^{2+} channel currents in rat cerebellar granule neurons. *J Neurosci* **15**, 2995–3012.

Schaefer AT, Helmstaedter M, Sakmann B & Korngreen A (2003) Correction of conductance measurements in non-space-clamped structures: 1. Voltage-gated K(+) channels. *Biophys J* **84**, 3508–3528.

Scott SH (2000). Population vectors and motor cortex: neural coding or epiphenomenon? *Nat Neurosci* **3**, 307–308.

Selinfreund RH & Blair LAC (1994). Insulin-like growth factor-1 induces a rapid increase in calcium currents and spontaneous membrane activity in clonal pituitary cells. *Mol Pharmacol* **45**, 1215–1220.

Shimokawa I, Higami Y, Utsuyama M, Tuchiya T, Komatsu T, Chiba T & Yamaza H (2002). Life span extension by reduction in growth hormone-insulin-like growth factor-1 axis in a transgenic rat model. *Am J Pathol* **160**, 2259–2265.

Smith CD, Umberger GH, Manning EL, Slevin JT, Wekstein DR, Schmitt FA, Markesbery WR, Zhang Z, Gerhardt GA, Kryscio RJ & Gash DM (1999). Critical decline in fine motor hand movements in human aging. *Neurology* **53**, 1458–1461.

Sonntag WE, Lynch C, Bennett SA, Khan AS, Thornton PL, Cooney PT, Ingram RL, Mcshane T & Brunso-Bechtold JK (1999). Alterations in insulin-like growth factor-1 gene and protein expression and type 1 insulin-like growth factor receptors in the brains of ageing rats. *Neuroscience* **88**, 269–279.

Sonntag WE, Lynch C, Thornton P, Khan A, Bennett S & Ingram R (2000). The effects of growth hormone and IGF-1 deficiency on cerebrovascular and brain ageing. *J Anat* **197**, 575–585.

Sonntag WE, Steger RW, Forman LJ & Meites J (1980). Decreased pulsatile release of growth hormone in old male rats. *Endocrinology* **107**, 1875–1879.

Stewart A & Foehring RC (2000). Calcium currents in retrogradely labeled pyramidal cells from rat sensorimotor cortex. *J Neurophysiol* **83**, 2349–2354.

Stewart AE & Foehring RC (2001). Effects of spike parameters and neuromodulators on action potential waveform-induced calcium entry into pyramidal neurons. *J Neurophysiol* **85**, 1412–1423.

Talley EM, Cribbs LL, Lee JH, Daud A, Perez-Reyes E & Bayliss DA (1999). Differential distribution of three members of a gene family encoding low voltage-activated (T-type) calcium channels. *J Neurosci* **19**, 1895–1911.

Todorov E (2000). Direct cortical control of muscle activation in voluntary arm movements: a model. *Nat Neurosci* **3**, 391–398.

Umemiya M & Berger AJ (1995). Single-channel properties of four calcium channel types in rat motoneurons. *J Neurosci* **15**, 2218–2224.

Velasco B, Cacicedo L, Melian E, Fernandez-Vazquez G & Sanchez-Franco F (2001). Sensitivity to exogenous GH and reversibility of the reduced IGF-I gene expression in aging rats. *Eur J Endocrinol* **145**, 73–85.

Westenbroek RE, Hoskins L & Catterall W A (1998). Localization of Ca^{2+} channel subtypes on rat spinal motor neurons, interneurons and nerve terminals. *J Neurosci* **18**, 6319–6330.

Wolkow CA, Kimura KD, Lee MS, Ruvkun G (2000). Regulation of *C. elegans* life-span by insulinlike signaling in the nervous system. *Science* **5489**, 147–150.

Ye P, Li L, Richards RG, Diaugustine RP & D'Ercole AJ (2002). Myelination is altered in insulin-like growth factor-I null mutant mice. *J Neurosci* **22**, 6041–6051.

Zheng Z, Wang ZM & Delbono O (2002*a*). Insulin-like growth factor-1 increases skeletal muscle DHPR alpha 1S transcriptional activity by acting on the cAMP-response element-binding protein element of the promoter region. *J Biol Chem* **277**, 50535–50542.

Zheng Z, Wang Z-M & Delbono O (2002*b*). Charge movement and transcription regulation of L-type calcium channel alpha-1S in skeletal muscle cells. *J Physiol* **540**, 397–409.

Acknowledgements
The present study was supported by the National Institutes of Health/National Institute on Aging (AG18755, AG13934, and AG15820), and Muscular Dystrophy Association of America grants to Osvaldo Delbono.